LIQUID CRYSTALS, 2001, VOL. 28, NO. 9, 1415–1423

A new series with smectic blue phases and SmC*–BP_{Sm2} direct transition

C. DA CRUZ, E. GRELET†, J. C. ROUILLON, J. P. MARCEROU, G. SIGAUD, B. PANSU† and H. T. NGUYEN*

Centre de Recherche Paul Pascal, Université de Bordeaux, I, Avenue A. Schweitzer, F-33600 Pessac, France

†Laboratoire de Physique des Solides, Université Paris-Sud, 91405 Orsay Cedex, France

(*Received 17 March 2001; accepted 17 April 2001*)

A series of trifluoro-substituted benzoate derivatives: (*R*)-1-methylheptyl 4-[4-(4-alkyloxy-3-fluorobenzoyloxy)-3-fluorobenzoyloxy]-3-fluorobenzoates is reported. The short chain members ($n = 8$ to 12) display the phase sequence Cr–SmC*–TGBC–TGBA–BP_{Sm}–I (except for $n = 8, 9$ where there is no TGBC phase), whereas for the longer ones ($n = 13, 14, 16$) a direct SmC*–BP_{Sm2} transition is observed for the first time. We observe for $n = 8$ to 10, BP_{Sm1} and BP_{Sm3}; for $n = 11$, the full set of three BP_{Sm} phases, and for $n > 11$, only BP_{Sm2} and BP_{Sm3} phases. The mesomorphic properties were studied by optical microscopy, DSC, and electro-optical, optical rotatory power and X-ray scattering measurements. The effect of the positions of fluorine atoms and their influence over mesomorphic behaviour are discussed.

1. Introduction

The twist grain boundary, TGB, phases and the blue phases, BPs, are two kinds of frustrated phase containing chiral molecules, resulting from a competition between the chiral forces and the tendency for the molecules to pack in such a way that they fill space uniformly.

The existence of the twist grain boundary smectic A (TGBA) phase in chiral systems was predicted by Renn and Lubensky [1] from the De Gennes model [2] and first demonstrated experimentally by Goodby *et al.* in 1989 [3, 4]. The TGBA phase structure involves slabs of SmA material stacked regularly in a helical fashion along an axis parallel to the smectic layers. Adjacent slabs are connected continuously via a grain boundary which consists of a grid of parallel equispaced screw dislocation lines which allow helical twisting. This periodic ordering of screw dislocations relieves the frustration of the molecules which need to form a helical structure. TGBC and TGBC* phases in which the smectic slabs are, respectively, SmC and SmC* [5, 6], were also predicted and the existence of the TGBC phase was demonstrated by the Bordeaux group [7].

Blue phases were exhibited by the first liquid crystalline material (cholesteryl benzoate) to be discovered [8]. The recognition that BPs are distinct thermodynamically stable phases, however, was only made in the 1970s [9]. BPs are normally found between the isotropic liquid state and a cholesteric phase of sufficiently short pitch in the phase sequence I–BPs–N*, except in two cases for which direct BPI–SmA transitions have been observed [10, 11]. In order of increasing temperature, they are termed blue phase I (BPI), blue phase II (BPII) and blue phase III (BPIII). BPI and BPII are cubic phases and have body centred cubic and simple cubic symmetry, respectively. BPIII seems to have an amorphous structure of the same macroscopic symmetry as the isotropic phase [12]. In models of cubic blue phases, the basic unit is thought to be a double twist tube without a real experimental meaning, in the sense that there is no density modulation in the unit cell. These tubes have been shown theoretically to be more stable than the single twist structure of the N* phase at higher temperatures and when the chirality of the molecules is sufficiently high for the helical pitch to be short enough. In 1997, the Bordeaux group reported a new phase sequence, I–BPs–TGBA in a chiral tolane series and in the absence of any cholesteric phase behaviour [13]. These BPs were shown not to be classical in structure but instead were termed smectic BP_{Sm} possessing a smectic-like ordering.

A similar phase sequence is observed in the series:

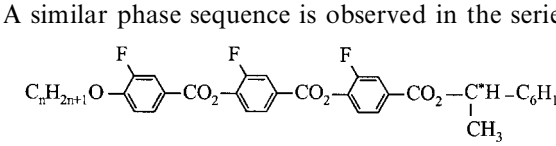

(*R*) Series I

*Author for correspondence; e-mail: tinh@crpp.u-bordeaux.fr

Liquid Crystals ISSN 0267-8292 print/ISSN 1366-5855 online © 2001 Taylor & Francis Ltd
http://www.tandf.co.uk/journals
DOI: 10.1080/02678290110066822

but they exhibit a larger BP_{Sm} temperature range. The long chain derivatives ($n > 12$) exhibit a new mesomorphic behaviour with a direct SmC*–BP_{Sm2} transition without the presence of any TGB phase. Here we report the detailed investigations of all members of this series and specifically their synthesis, mesomorphic properties, electro-optical properties with optical rotatory power and X-ray scattering measurements.

2. Synthesis and mesomorphic properties

The materials studied in this paper were synthesized according to the scheme. The 4-alkyloxy-3-fluorobenzoic acids and 4-benzyloxy-3-fluorobenzoic acid were prepared using well known methods [14, 15].

Phase sequences were determined from texture observations made on conventional thin samples by polarizing optical microscopy (POM) (Leitz Ortholux microscope equipped with a Mettler FP5 hot stage). The phase transition temperatures and associated enthalpies were evaluated from DSC studies (Perkin-Elmer DSC7). Typical DSC plots for different homologues of the series are shown in figure 1. The mesomorphic properties of all the newly synthesized compounds are collected in table 1. The phase transition temperatures and enthalpies were determined on heating. All compounds of the series for $n = 8$ to 16 are mesogenic. Blue phases are present over the whole series. The temperature for transition to the isotropic phase increases until $n = 12$ and then decreases.

We could detect by POM the presence of a TGBA phase (whose nature was determined by X-ray scattering) for the compounds $n = 9$–12. For the longest chains ($n = 13, 14, 16$), a direct SmC*–BP_{Sm} transition was observed for the first time and studied by electro-optical measurements.

Different behaviours are present, for the short chain members ($n < 10$) the phase sequence is Cr–SmC*–TGBA–BP_{Sm1}–BP_{Sm3}–I (with a TGBC phase for $n = 10$), while for the long chain members ($n \geqslant 13$) it is Cr–SmC*–BP_{Sm2}–BP_{Sm3}–I. The compound with $n = 11$ exhibits all the phases, Cr–SmC*–TGBC–TGBA–BP_{Sm1}–BP_{Sm2}–BP_{Sm3}–I and the compound with $n = 12$ exhibits the phase sequence Cr–SmC*–TGBC–TGBA–BP_{Sm2}–BP_{Sm3}–I. One notes the occurrence of an additional phase for the intermediate chain lengths ($n = 10$–12). This phase, which extends over a narrow temperature range, is evidenced by two peaks in the thermograms (see figure 1). This double event is observed only upon heating, and a single peak is recovered upon cooling: this behaviour is strongly reminiscent of the SmC*–TGBC–TGBA phase sequence characterized in a former series [13]. This, together with the evolution of the layer spacing, leads us to assign this intermediate phase as TGBC.

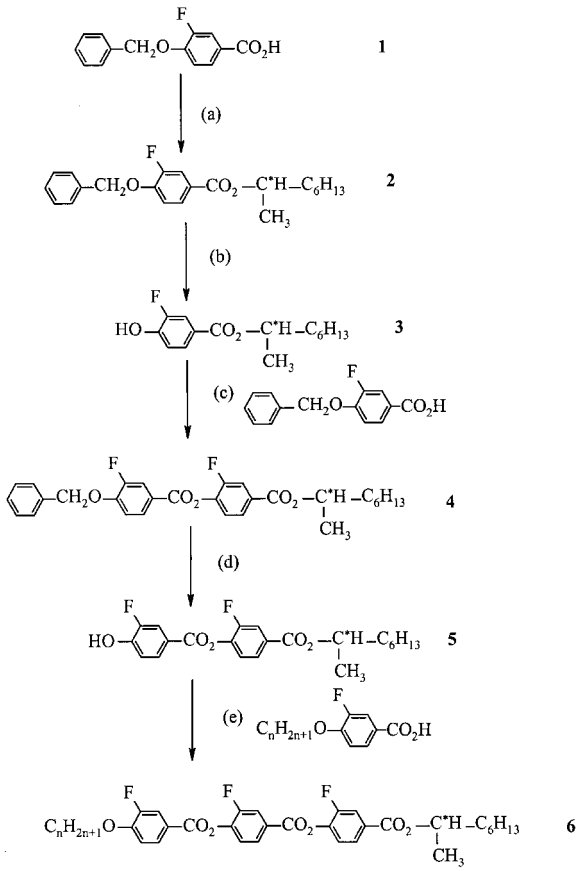

a HO-C*H(CH_3)-C_6H_{13}, DCC, DMAP, CH_2Cl_2.
b, d H_2, Pd/C, ethyl acetate.
c, e DCC, DMAP, CH_2Cl_2.

Scheme.

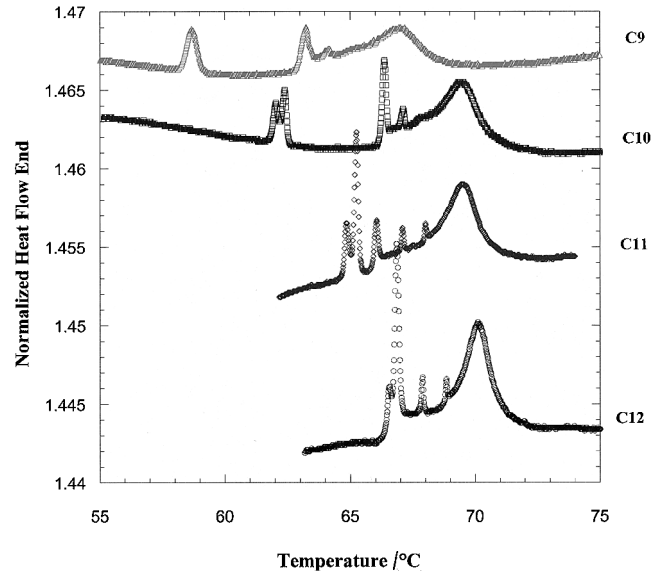

Figure 1. DSC thermograms of different compounds of the series ($n = 9$ to 12) on heating at 0.2°C min^{-1}.

Table 1. Transition temperatures (°C) determined on heating and enthalpies in brackets (kJ mol^{-1}) of the series measured at the rate 0.2°C min^{-1}, except for the Cr–SmC* transition (1°C min^{-1}).

n	Cr		SmC*		TGBC		TGBA		BP$_{Sm1}$		BP$_{Sm2}$		BP$_{Sm3}$		I
8[e]	•	52.5 (9.03)	•	65.7	—		•	66.1	•		—		•	68.5	•
9	•	61.6 (36.38)	•	[58.7][d]	—		•	63.2	•		—	64.1 (1.78)[b]	•	66.9	•
10[e]	•	55 (24.1)	•	62.0 (0.28)[a]	•	62.4	•	66.4	•		—	67.1 (2.26)[b]	•	69.4	•
11	•	60.0 (43)	•	64.8 (0.55)[a]	•	65.2	•	66	•	67	•	68 (2.21)[b]	•	69.4	•
12	•	57.7 (39.27)	•	66.6 (0.63)[a]	•	66.9	•	67.9	—		•	68.8 (1.43)[b]	•	70.1	•
13	•	59.7 (39.13)	•	66.3	—		—		—	(2.8)[c]	•		•	68.7	•
14	•	58 (39.44)	•	66.3	—		—		—	(3.6)[c]	•		•	68.4	•
16	•	51.1 (53.6)	•	67.1	—		—		—	(4.0)[c]	•		•	68.5	•

[a] Sum of the enthalpies for the transitions SmC*–TGBC and TGBC–TGBA.
[b] Sum of the enthalpies for the transitions TGBA–BP$_{Sm1}$, BP$_{Sm1}$–BP$_{Sm2}$, BP$_{Sm2}$–BP$_{Sm3}$, BP$_{Sm3}$–I when these phases exist.
[c] Sum of the enthalpies for the transitions SmC*–BP$_{Sm2}$, BP$_{Sm2}$–BP$_{Sm3}$, BP$_{Sm3}$–I.
[d] Monotropic phases.
[e] Ferrielectric phases, enantiotropic for $n = 8$ (56°C on heating) and monotropic for $n = 10$ (47°C).

A general trend appears to be that there exists a temperature range of frustrated phases (TGBA and BP$_{Sm}$) which decreases from 8°C for $n = 9$ to 3°C for $n = 12$, and at the same time TGBA and BP$_{Sm1}$ disappear while BP$_{Sm2}$ appears. The temperature range of the TGBA phase is 5°C for $n = 9$ (without recrystallization), 4°C for $n = 10$, 0.8°C for $n = 11$, and 1°C for $n = 12$. We notice that for $n = 10$ and 11, the transition temperatures are almost the same between the TGBA phase and the BP$_{Sm}$ phases. Also, the sum of the enthalpies associated with the transitions TGBA–BP$_{Sm1}$, BP$_{Sm1}$–BP$_{Sm2}$, BP$_{Sm2}$–BP$_{Sm3}$ and BP$_{Sm3}$–I are the same (2.2 kJ mol^{-1}). However, the TGBA phase is more stable for the compound $n = 10$ (4.2°C) than for $n = 11$ (0.8°C). There is possibly a connection with the presence of the monotropic ferrielectric phases seen in compound $n = 10$ at 47°C on cooling. We also note that we cannot distinguish a BP$_{Sm2}$ phase in the compound $n = 10$ using DSC. The existence of a BP$_{Sm2}$ phase seems to occur only starting from the compound with $n = 11$, the differentiation between BP$_{Sm1}$ and BP$_{Sm2}$ is obtained using other techniques reported in this paper. For example, for a non-oriented sample a flat 100 μm capillary tube observed by POM, an increasing coloration in the BP$_{Sm1}$ phase occurs because it has a high optical rotatory power. On decreasing the temperature, the BP$_{Sm2}$ phase appears with a platelet texture, this seems to be in agreement with the peaks observed by DSC and with the assignment of a BP$_{Sm2}$ phase in this compound. In addition optical rotatory power (ORP) measurements and X-ray scattering studies show unambiguously the presence of the BP$_{Sm2}$ phase. For these optical observations we used an Olympus BH 2 BHS microscope equipped with a modified Linkam THM S600 heating stage regulated by a LakeShore 330 Temperature Controller. The main feature of this optical hot stage is a 0.02°C accuracy in temperature and a good control of the cooling (or heating) rate. This rate must be very low to be sure that all the phases nucleate and to obtain large monodomains: it is typically 0.001°C min^{-1}.

For the different compounds of the series, the temperature range for the crystalline BP$_{Sm}$ phases is around 1°C: 0.7°C ($n = 10$, BP$_{Sm1}$), 0.9°C ($n = 9$, BP$_{Sm1}$), 1°C ($n = 11$, BP$_{Sm1}$), 1°C ($n = 11$, BP$_{Sm2}$), 0.9°C ($n = 12$, BP$_{Sm2}$); this is a large temperature range for blue phases. The BP$_{Sm2}$ phase presents a typical texture with platelets, as shown in figure 2 in which large monodomains have been grown from the isotropic BP$_{Sm3}$ phase for the compound $n = 13$.

3. Electro-optical studies

Electro-optical properties were studied using the SSFLC configuration to evaluate polarization, response time, and tilt angle in a single set-up. Commercial cells (EHC, Japan) coated with indium tin oxide and rubbed polyimide were used. The thickness of the cells was around 15 μm, and the active area was 0.25 cm^2. A slow cooling from the isotropic phase through the frustrated phases (0.1°C min^{-1}) to the SmC* phase gave planar alignment. Alignment was better without the presence

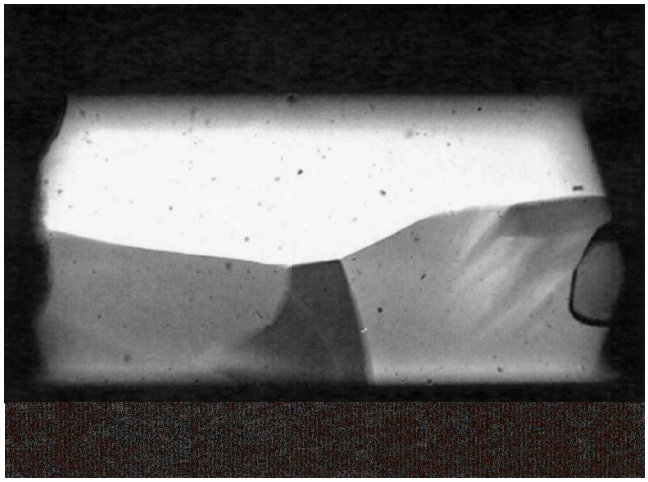

Figure 2. Single BP_{Sm2} monodomains grown from the BP_{Sm3} phase seen in transmission between crossed polarizers for the compound $n = 13$. The sample thickness is 100 μm.

of the TGBA phase. The compounds with $n = 10$, 13, and 14 were studied. The field used was a rectangular a.c. field of 4.6, 2.2 and 3.25 V μm^{-1}, for $n = 10$, 13, and 14, respectively. A frequency of 41 Hz was used for the measurements of polarization and electric response time and 0.1 Hz for the tilt angle. The polarization was calculated by the integration of the switching current under a rectangular a.c. field and the apparent tilt angle θ of the molecules from the smectic layer normal was calculated from the difference in the extinction positions between crossed polarizers under opposite unwinding fields. Well aligned samples were needed for the measurements of θ.

For the three compounds under test, the polarization values are very similar and more or less the same between $T = 55$°C and $T = 65$°C (figure 3). At the higher temperature phase transition the three polarizations tend to around 60 nC cm^{-2}, a high and unusual value due perhaps to the first order character of the phase transition. The polarization behaviour versus temperature is typical, i.e. polarization diminishes with increasing temperature. The maximum value for polarization is around 120 nC cm^{-2} at $T = 40$°C, similar to that measured for the compound with $n = 10$ of the analogous series without the fluorine in position 3 of the first phenyl ring near the chiral carbon [14].

The apparent tilt angle for $n = 10$ decreases from 30° to 22° on heating, in the typical way, and θ is more or less proportional to P (figure 4).

The electric response time curves (figure 5) show no anomalies, they decrease with increasing temperature due to the classical thermal behaviour of the viscosity of the compounds. When normalized at an applied field of 1 V μm^{-1}, figure 5 shows that this response time reaches 500 μs V μm^{-1} at 5°C below the higher phase transition.

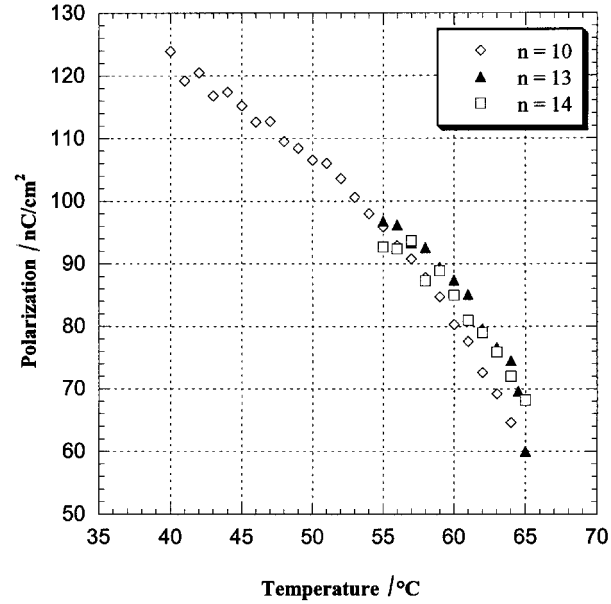

Figure 3. Temperature dependence of the polarization at saturation compared for the three compounds with $n = 10$ ($E = 4.6$ V μm^{-1}), $n = 13$ ($E = 2.2$ V μm^{-1}), $n = 14$ ($E = 3.25$ V μm^{-1}) at $\nu = 41$ Hz.

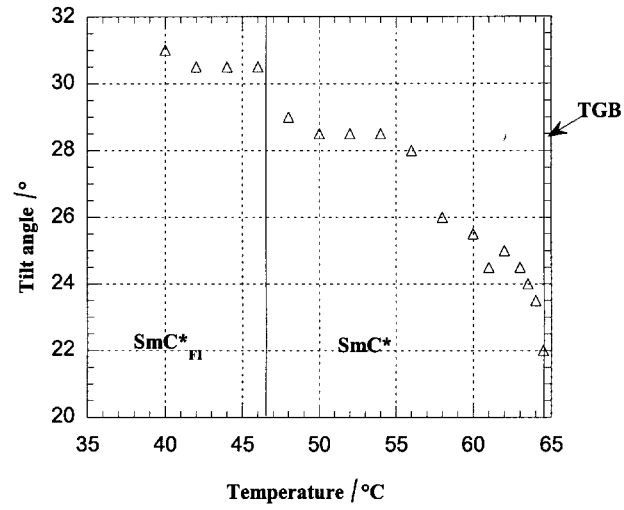

Figure 4. Temperature dependence of the apparent tilt angle ($E = 4.6$ V μm^{-1}, $\nu = 0.1$ Hz) for the $n = 10$ compound.

4. Optical rotatory power

We performed optical rotatory power measurements in the isotropic phase and when possible in the blue phases at the wavelength, λ, of 632.8 nm for the compound with $n = 10$ (figure 6) and at $\lambda = 632.8$ nm (red) and 543.5 nm (green) for the compounds $n = 11$ (figure 7) and $n = 14$ (figure 8) on a 2.5 mm thick cell. We notice a shift between the DSC and ORP temperatures for the phase transitions of about 2°C and so we shifted the ORP curves according to DSC temperatures.

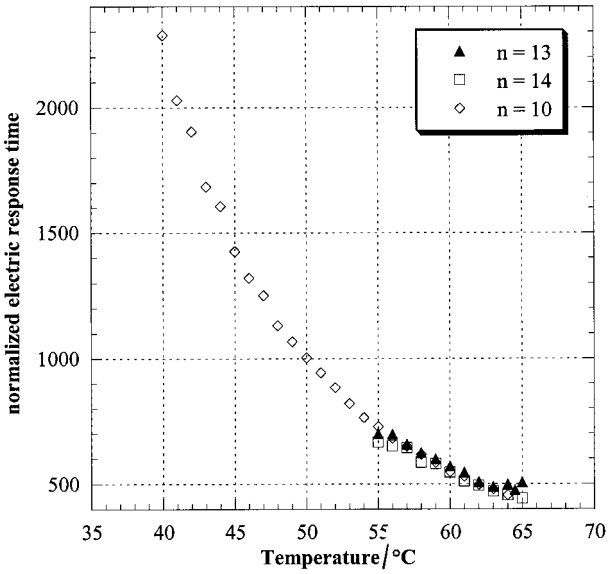

Figure 5. Temperature dependence of the electric response time for compounds with $n = 10$ ($E = 4.6$ V μm^{-1}, $\nu = 41$ Hz), $n = 13$ ($E = 2.2$ V μm^{-1}, $\nu = 41$ Hz) and $n = 14$ ($E = 3.25$ V μm^{-1}, $\nu = 41$ Hz).

The general trend is that for (*R*) compounds starting from the isotropic phase and on cooling, one first measures a negative ORP up to $-3°\,\mathrm{mm}^{-1}$ due to the approach of the BP$_{Sm3}$ phase, then a positive contribution occurs, due to the other BP$_{Sm}$ phases. There is a perfect extinction in the BP$_{Sm3}$ phase leading to an accuracy better than $0.1°\,\mathrm{mm}^{-1}$. By contrast in the BP$_{Sm2}$ phase, the search of the direction of polarization fails due to the polycrystalline character of the sample and to its slight birefringence (in agreement with X-ray results). Eventually in the BP$_{Sm1}$ phase the birefringence is sufficiently low to allow measurements; we get a minimum of light and this time an accuracy about $2°\,\mathrm{mm}^{-1}$ A polycrystallinity remains that seems to diminish with time (see figure 7 in which the results show no saturation).

We have tried to fit the results with respect to the light wavelength in the high temperature region. Empirically we find a λ^{-3} law works well. The classic theory $\rho = A_2\lambda^{-2}$ [16, 17] should not apply in this case as the light wavelength is not much greater than the helical pitch.

5. X-ray scattering

X-ray diffraction experiments were performed on the compound $n = 10$ to determine the layer thickness in the TGB phase and its dependence upon temperature (figure 9). The layer thickness in the TGB phase was found to be around 37.5 Å, remains constant as the temperature varied. This behaviour shows that this phase should be a TGBA phase [7].

In contrast to classic blue phases, smectic blue phases exhibit rather long range smectic order that can be studied by X-ray scattering. It has been shown that in these phases the smectic order is strongly correlated with the orientational 3D order and is therefore, enhanced in some directions linked with the orientational symmetry [18, 19]. These directions are revealed by the presence of peaks in the diffuse smectic ring. Thus, the angular distribution of these peaks gives information on the symmetry of the orientational cell. Experiments have been performed on monodomains of smectic blue phase

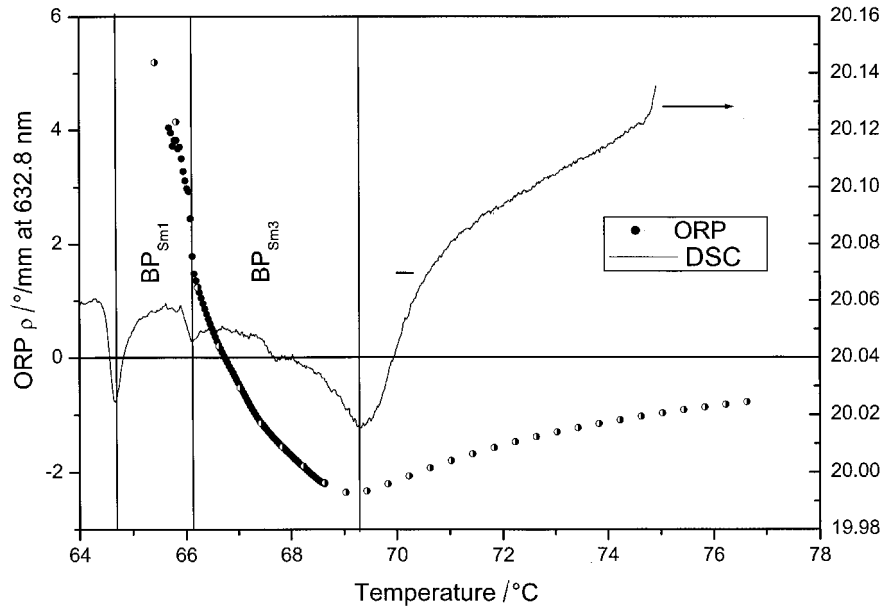

Figure 6. Optical rotary power at 632.8 nm in a 2.5 mm thick sample of the $n = 10$ compound.

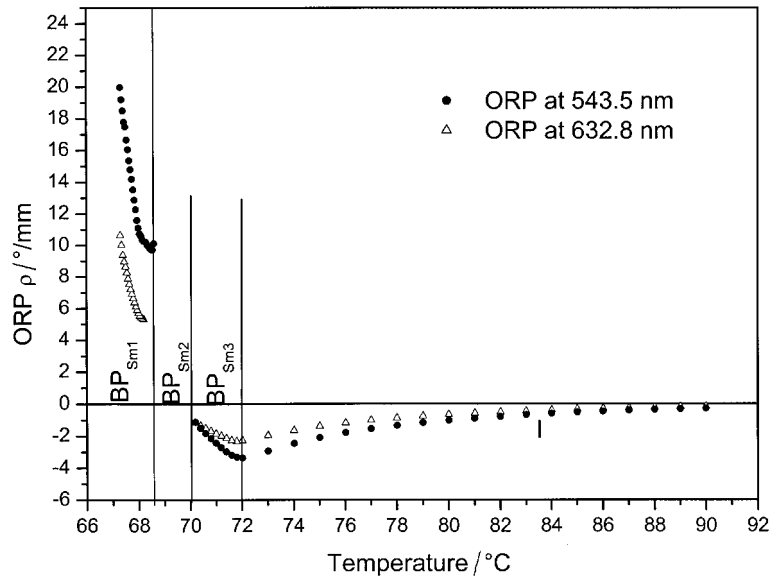

Figure 7. Optical rotary power at 632.8 nm and 543.5 nm in a 2.5 mm thick sample of the $n = 11$ compound.

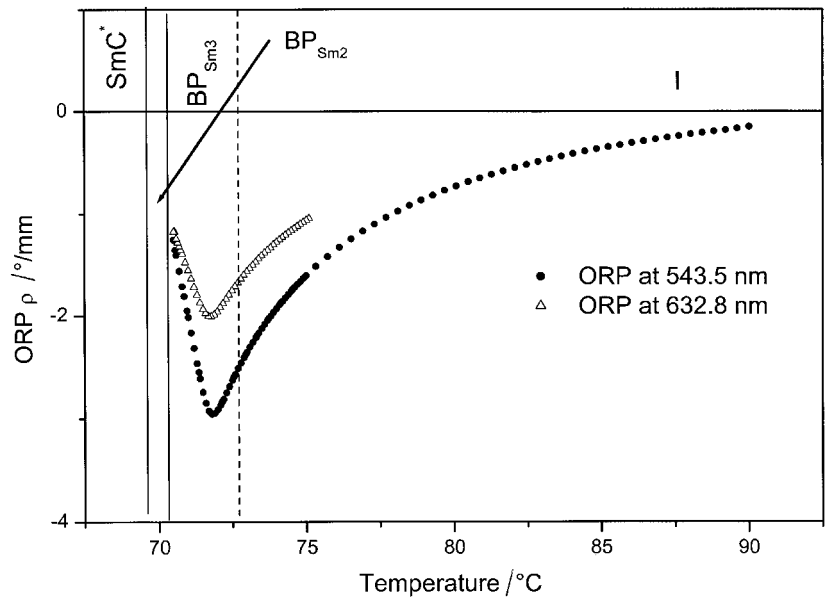

Figure 8. Optical rotary power at 632.8 nm and 543.5 nm in a 2.5 mm thick sample of the $n = 14$ compound.

BP_{Sm2} shown by compound $n = 13$. One monodomain has been grown *in situ* in an X-ray glass capillary placed in the centre of a hot stage, transparent to X-rays. A very slow cooling rate from the isotropic phase to the BP phase is necessary to grow one domain larger than the beam size (0.5 mm).

X-ray scattering experiments were performed in Lure (Orsay, France) using synchrotron radiation. Different scattering patterns were recorded on the imaging plates as the capillary was rotated by steps of 15° (angle β) around the vertical axis between two consecutive scans (figure 10) [18]. Each pattern exhibits a diffuse ring which is not homogeneous. For each value of β, the intensity $I(\beta, \mu)$ along the smectic ring can be analysed as a function of the angle μ with respect to the vertical axis (table 2). Thus, the set of data $I(\beta, \mu)$ gives information on the whole reciprocal space and therefore on the directions of the smectic enhancements.

Four pairs are observed. The most intense one is referred to as P0, the three others were denoted P1, P2, P3. Table 3 shows that the three directions, P1, P2, P3, are perpendicular to P0. Thus, these three directions are in the same plane and separated by angles close to 120°. This proves the existence of at least a three-fold axis in the orientational cell and that quasi long range smectic order is observed not only along this axis (P0) but also along three axes perpendicular to it (P1, P2, P3). It is important to note that this scattering is on the scale of

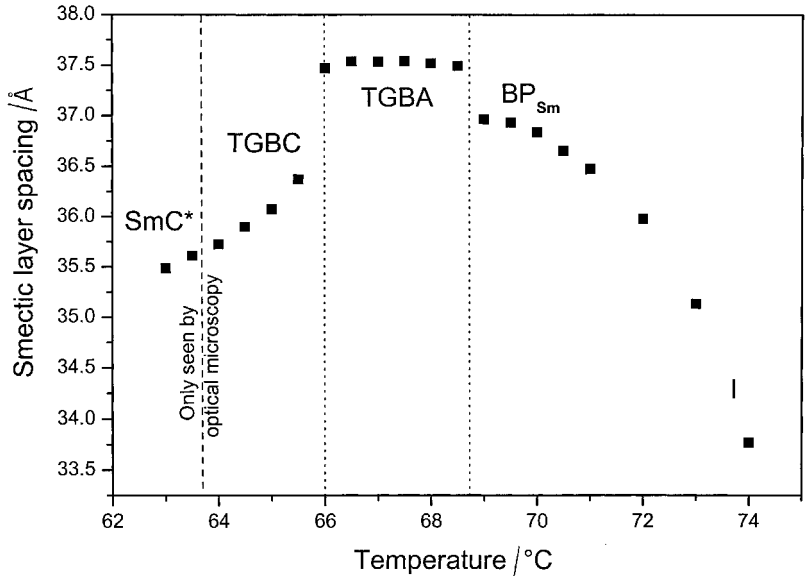

Figure 9. Layer thickness versus temperature for the $n = 10$ compound.

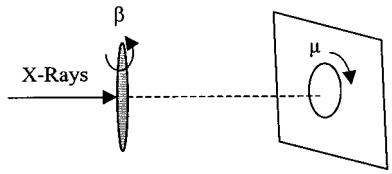

Figure 10. Experimental set-up for X-ray scattering.

Table 2. Position of the four peaks P0, P1, P2, P3.

	Angle/°	
Peak	β	μ
P0	155	7
P1	−146	−69
P2	−119	27
P3	−22	−92

Table 3. Angles (degrees) between the directions along which the peaks are observed.

	P0	P1	P2	P3
P0	0	93	88	91
P1	93	0	117	120
P2	88	117	0	123
P3	91	120	123	0

the smectic order and does not give any information on the value of the orientational cell parameter which is on the scale of the pitch. This is reminiscent of the BP_{Sm2} structure observed already in other compounds [18]. The symmetries exhibited by these patterns certainly reflect those of the three-dimensional unit cell of this phase. The experiments confirm that the smectic blue phase is hexagonal, BP_{Sm2}.

For the thermal dependence of the layer spacing, for compounds studied in the SmC* phase, we get the typical increase on heating compatible with the decrease of the tilt angle (figure 11).

6. Discussion and conclusion

The Bordeaux group has already reported a series exhibiting smectic blue phases having the general formula [13]:

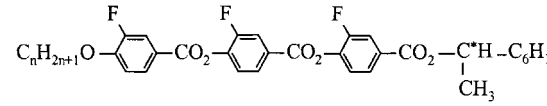

Series II

All the compounds of this series exhibit SmC*, TGBA, BP_{Sm2} and BP_{Sm3} phases, with the appearence of a TGBC phase for the compounds with $n > 12$ and a BP_{Sm1} phase for compounds $n = 14$, 16 and 18. The very short helical pitch due to the presence of the two fluorine atoms was certainly the reason for the direct transition from the TGBA to the blue phase in the absence of any cholesteric phase.

In addition, we have already reported [14] the effect of the presence of these two fluorine atoms on the properties of the structurally similar series, in which the tolane group is replaced by a benzoate group. The unfluorinated homologous series III is a pure 'anticlinic series'. The presence of the two fluorine atoms gives rise to the particular feature that the series displays both TGBA (longer chain members) and SmC^*_A phases (shorter chain members).

In series I reported here, we have introduced a third fluorine atom on position 3 of the phenyl ring near the chiral centre, which leads to the presence of smectic blue

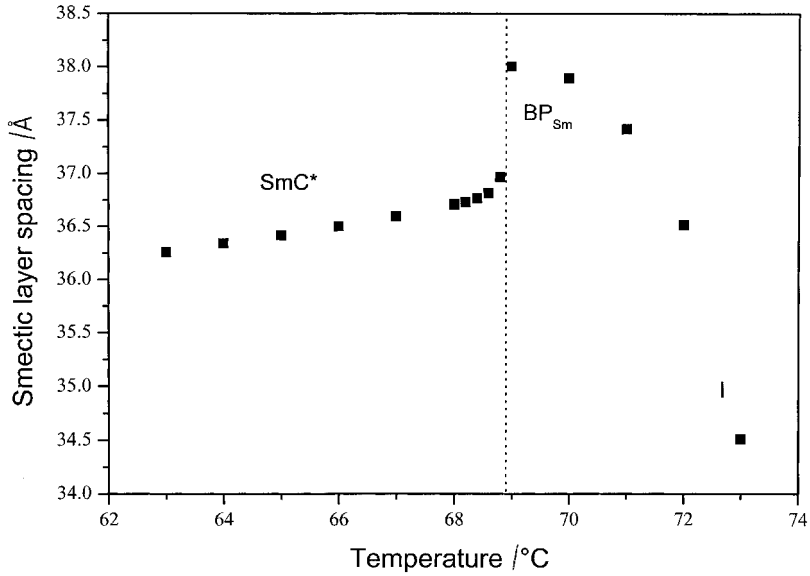

Figure 11. Layer thickness versus temperature for the $n = 13$ compound.

phases and also to a new phase transition, SmC*–BP_{Sm2}, on heating and cooling. The presence of a SmC* or a TGBA phase below the BP_{Sm2} phase seems to have no influence on the BP_{Sm2} symmetry (hexagonal).

7. Experimental

NMR spectra were recorded on a Bruker HW 300 MHz spectrometer; infrared spectra were recorded on a Perkin-Elmer 783 spectrophotometer. The following examples are typical of the synthetic methods used to obtain the compounds given in table 1.

7.1. *(R)-1-Methylheptyl 4-benzyloxy-3-fluorobenzoate* **2**

To a solution of (*R*)-2-octanol (3.9 g, 30 mmol) in CH_2Cl_2 (35 ml) was added DCC (6.18 g, 30 mmol), DMAP (0.3 g) and 4-benzyloxy-3-fluorobenzoic acid (7.4 g, 30 mmol). The resulting solution was stirred at room temperature overnight; it was filtered, and the solvent evaporated. The residue was chromatographed on silica gel with CH_2Cl_2 as eluent. The desired compound was used without further purification. Yield = 9 g (84%). ^{1}H NMR ($CDCl_3$, ppm): 0.9 (t, 3H, CH_3 of C_6H_{13}), 1.2–1.5 (m, 11H, $4CH_2$ and CH_3–CHO), 1.6–1.8 (m, 2H, $CH_2\beta$), 5.1 (m, 1H, O–CH–CH_2), 5.2 (s, 2H, CH_2–O), 7 (t, 1H arom. *meta* to F), 7.4 (m, 5H arom.), 7.8 (m, 2H arom. *ortho* and *para* to F).

7.2. *(R)-1-Methylheptyl 4-hydroxy-3-fluorobenzoate* **3**

To a solution of compound **2** (9 g, 25 mmol) dissolved in ethyl acetate (>200 ml) was added Pd/C (0.9 g). Hydrogen was added under a slight pressure. When the reaction was over, the catalyst was filtered off and the solvent evaporated. As the reaction is quantitative, the liquid phenol was used without further purification. Yield = 6.1 g (88%). ^{1}H NMR ($CDCl_3$, ppm): 0.9 (t, 3H, CH_3 of C_6H_{13}), 1.2–1.5 (m, 11H, $4CH_2$ and CH_3–CHO), 1.6–1.8 (m, 2H, $CH_2\beta$), 5.1 (m, 1H, O–CH–CH_2), 5.6 (s, 1H, O–H), 7 (t, 1H arom. *meta* to F), 7.8 (m, 2H arom. *ortho* and *para* to F).

7.3. *(R)-1-Methylheptyl 4-(4-benzyloxy-3-fluorobenzoyloxy)-3-fluorobenzoate:* **4**

To a solution of phenol **3** (4.0 g, 15 mmol) in CH_2Cl_2 (25 ml) was added DCC (3.5 g, 15 mmol), DMAP (0.15 g) and 4-benzyloxy-3-fluorobenzoic acid (3.8 g, 15 mmol). The resulting mixture was stirred at room temperature overnight. The solution was then filtered, and the solvent evaporated. The residue was chromatographed on silica gel using CH_2Cl_2 as eluent. The product (white powder) was used without further purification. Yield = 5.8 g (78%). ^{1}H NMR ($CDCl_3$, ppm): 0.9 (t, 3H, CH_3 of C_6H_{13}), 1.2–1.5 (m, 11H, $4CH_2$ of C_6H_{13} and CH_3–CHO), 1.6–1.8 (m, 2H, $CH_2\beta$), 5.1 (m, 1H, O–CH–CH_2–), 5.2 (s, 2H, –CH_2–O–), 7.1 (t, 1H arom. *meta* to F of the first ring), 7.4 (m, 6H arom., 5H arom. and 1H arom. *meta* to F of the second ring), 7.9 (m, 4H arom., 2H *ortho* and *para* to F of the first ring, 2H *ortho* and *para* to F of the second ring). IR (KBr) (cm^{-1}): 2955, 2931, 2857 (C–H aliphatic), 1734, 1714 (C=O), 1619, 1524, 1436 (C=C phenyl rings).

7.4. *(R)-1-Methylheptyl 4-(4-hydroxy-3-fluorobenzoyloxy)-3-fluoro benzoate* **5**

To a solution of compound **4** (5.8 g, 11.7 mmol) dissolved in ethyl acetate (>150 ml) was added Pd/C (0.6 g), and the mixture was stirred under a slight pressure

of hydrogen. The reaction over, the catalyst was filtered off and the solvent evaporated. The liquid phenol was used without further purification. Yield = 4 g (84.2%). ^{1}H NMR ($CDCl_3$, ppm): 0.9 (t, 3H, CH_3 of C_6H_{13}), 1.2–1.5 (m, 11H, $4CH_2$ of C_6H_{13} and CH_3–CHO), 1.6–1.8 (m, 2H, $CH_2\beta$), 5.15 (m, 1H, O–CH–CH_2–), 5.8 (large s, 1H, O–H), 7.2 (t, 1H arom. *meta* to F of the first ring), 7.3 (m, 1H arom. *meta* to F of the second ring), 7.9 (m, 4H arom., 2H *ortho* and *para* to F of the first ring, 2H *ortho* and *para* to F of the second ring).

7.5. *(R)-1-Methylheptyl 4-[4-(4-decyloxy-3-fluorobenzoyloxy)-3-fluorobenzoyloxy]-3-fluorobenzoate* ***6***

4-Decyloxy-3-fluorobenzoic acid (0.15 g, 0.5 mmol) was added to a solution of phenol **5** (0.21 g, 0.5 mmol), DCC (0.12 g, 0.5 mmol), DMAP (0.005 g) in CH_2Cl_2 (5 ml). The mixture was stirred overnight at room temperature; it was filtered, and the solvent evaporated. The residue was purified by chromatography on silica gel using toluene as eluent. The product was crystallized from absolute ethanol. Yield = 0.18 g (52.6%). ^{1}H NMR ($CDCl_3$, ppm): 0.8–1 (m, 6H, CH_3 of C_6H_{13} and CH_3 of $C_{10}H_{21}$), 1.2–1.5 (m, 22H, $7CH_2$ of $C_{10}H_{21}$, $4CH_2$ of C_6H_{13}), 1.6–1.8 (m, 6H, $2CH_2\beta$), 4.1 (t, 2H, –CH_2–O), 5.1 (m, 1H, O–CH–CH_2–), 7.1 (t, 1H arom. *meta* to F of the first ring), 7.35 (t, 1H arom. *meta* to F of the second ring), 7.45 (t, 1H arom. *meta* to F of the third ring), 8 (m, 6H arom., 2H *ortho* and *para* to F of the first ring, 2H *ortho* and *para* to F of the second ring, 2H *ortho* and *para* to F of the third ring). IR (KBr) (cm^{-1}): 2957, 2928, 2853 (C–H aliphatic), 1742, 1720 (C=O), 1616, 1510, 1444 (C=C phenyl rings).

One of us, C. Da Cruz, wishes to thank Praxis XXI for financial support.

References

[1] Renn, S. R., and Lubensky, T. C., 1988, *Phys. Rev. A*, **38,** 2132.

[2] De Gennes, P. G., 1972, *Solid State Commun.*, **10,** 753.

[3] (*a*) Goodby, J. W., Waugh, M. A., Stein, S. M., Chin, E., Pindak, R., and Patel, J. S., 1989, *Nature*, **337,** 449; (*b*) Goodby, J. W., Waugh, M. A., Stein, S. M., Chin, E., Pindak, R., and Patel, J. S., 1989, *J. Am. chem. Soc.*, **111,** 8119.

[4] Srajer, G., Pindak, R., Waugh, M. A., Goodby, J. W., and Patel, J. S., 1990, *Phys. Rev. Lett.*, **64,** 1545.

[5] Renn, S. R., and Lubensky, T. C., 1991, *Mol. Cryst. liq. Cryst.*, **209,** 349.

[6] Renn, S. R., 1992, *Phys. Rev. A*, **45,** 953.

[7] Nguyen, H. T., Bouchta, A., Navailles, L., Barois, P., Isaert, N., Twieg, R. J., Maaroufi, A., and Destrade, C., 1992, *J. Phys. II Fr.*, **2,** 1889.

[8] Reinitzer, 1888, *Monatsh. Chem.*, **9,** 421.

[9] (*a*) Coates, D., and Gray, G. W., 1973, *Phys. Lett.*, **45A,** 115; (*b*) Armitage, D., and Price, F. P., 1976, *J. appl. Phys.*, **47,** 2735.

[10] Onusseit, H., and Stegemeyer, H., 1984, *Z. Naturforsch.*, **39a,** 658.

[11] Nguyen, H. T., Salleneuve, C., Babeau, A., Galvan, J. M., and Destrade, C., 1987, *Mol. Cryst. liq. Cryst.*, **154,** 147.

[12] Kutnjak, Z., Garland, C. W., Passmore, J. L., and Collings, P. J., 1995, *Phys. Rev. Lett.*, **74,** 4859.

[13] Li, M. H., Laux, V., Nguyen, H. T., Sigaud, G., Barois, P., and Isaert, N., 1997, *Liq. Cryst.*, **23,** 389.

[14] Da Cruz, C., Rouillon, J. C., Marcerou, J. P., Isaert, N., and Nguyen, H. T., 2001, *Liq. Cryst.*, **28,** 125.

[15] Nabor, M. F., Nguyen, H. T., Destrade, C., Marcerou, J. P., and Twieg, R. J., 1991, *Liq. Cryst.*, **10,** 785.

[16] Bensimon, D., Domany, E., and Shtrikman, S., 1983, *Phys. Rev. A*, **28,** 427.

[17] Ennis, J., Wyse, J. E., and Collings, P. J., 1989, *Liq. Cryst.*, **5,** 861.

[18] Pansu, B., Grelet, E., Li, M. H., and Nguyen, H. T., 2000, *Phys. Rev. E*, **62,** 658.

[19] Grelet, E., Pansu, B., Li, M. H., and Nguyen, H. T., *Phys. Rev. Lett.* (in the press).